

# DILEPTON PRODUCTION AND CHIRAL SYMMETRY

V. KOCH<sup>1</sup>, M. BLEICHER<sup>1</sup>, A.K. DUTT-MAZUMDER<sup>2</sup>, C. GALE<sup>2</sup>,  
C.M. KO<sup>3</sup>

(1) *Lawrence Berkeley National Laboratory, Berkeley, CA 94720*

(2) *McGill University, Montreal, Quebec H3A, Canada*

(3) *Texas A&M University, College Station, TX 77843, USA*

## Abstract

We discuss how dilepton production is related to chiral symmetry and its restoration. We then analyse presently available data by the CERES collaboration in this context. We find that the present data do not support any conclusions concerning the restoration of chiral symmetry. We finally provide a prediction for the dilepton spectrum for the just completed low energy (40 GeV) run at the SPS.

## 1 Introduction

Electromagnetic probes provide a unique tool to investigate the early and interior properties of the system created in a heavy ion collision. Dileptons are of particular interest as their production cross section is related to the correlation function of the iso-vector vector current, the conserved current of the  $SU_R(2) \times SU_L(2)$  chiral symmetry. Thus, a careful study of the dilepton spectrum may provide some evidence and signal for the existence of a chirally restored phase created in a heavy ion collisions. Of course, unambiguous proof of chiral restoration requires the measurement of both iso-vector vector and iso-vector axial-vector correlation functions. The detection of the latter, however, is rather difficult, as it does not couple to a penetrating probe but rather to pionic degrees of freedom, and thus is strongly affected by final state interactions. However, at least at low temperatures one can show [1], that the onset of chiral restoration goes via the mixing of the vector and axial correlators. Assuming that this mixing is the dominant mechanism for chiral restoration (for a discussion of other possibilities see e.g. [2]), one expects considerable changes in the vector-correlator, which is measurable via dilepton production.

Let us, however, already note at this point that the medium can not only give rise to mixing of vector and axial vector correlation functions in the iso-vector channel, but also to mixing between iso-scalar and iso-vector ( $\rho$  and  $\omega$ ) correlator. This mixing is *not* related to chiral restoration, but certainly contributes to the dilepton spectrum, as both iso-vector and iso-scalar currents couple to the electromagnetic field. For the purpose of extracting information about possible chiral restoration, it has to be considered as ‘background’.

## 2 Chiral restoration and mixing

As already mentioned in the introduction, to leading order in the temperature the iso-vector vector correlator receives an admixture from the axial correlator [1]. Similar arguments, although somewhat model dependent, can also be given at finite density, where one again finds this mixing of vector and axial vector correlator [3]. In more physical terms, in both cases a pion from either the heat bath (finite temperature) or from the pion cloud of the nucleons (finite density) couples to the vector-current ( $\rho$  meson) to form an axial-vector ( $a_1$  or pion) intermediate state. This is depicted schematically on the left hand side of fig. 1. Conversely, the pions from the heatbath and/or pion cloud also give rise to a vector-admixture to the axial-vector correlator. One, therefore, can imagine that a certain temperature/density vector and axial-vector correlators are fully mixed and thus indistinguishable, which in turn means that chiral symmetry is restored.

The pions in the medium, however, also give rise to other mixing. For example a pion from the heatbath may couple to a  $\rho$ -meson to give an  $\omega$  intermediate state. This corresponds to the mixing between the iso-vector vector and iso-scalar vector correlators. This process is depicted schematically on the right hand side of fig. 1. This mixing is *not* related to chiral symmetry restoration, but still affects the dilepton spectrum.

The contribution of these mixings to the dilepton spectrum can be easily understood in simple physical terms. The dilepton-production cross section is proportional to the imaginary part of these correlation functions, which corresponds to a simple cut of the diagrams depicted in fig.1. Therefore, the matrix-elements responsible for vector axial-vector mixing are identical to those for the Dalitz-decay of the  $a_1$ -meson. A similar relation hold between the the mixing of iso-vector and iso-scalar correlators to the Dalitz decay of the  $\omega$  meson.

In other words, the contribution of the  $a_1$ -Dalitz decay to the total dilepton spectrum provides a measure for the importance of the vector axial-vector mixing, i.e. for the sensitivity to chiral restoration effects. While it might be

impossible to extract this channel from the data, in a given model calculation it can be easily accessed. We will show below, that the  $a_1$ -Dalitz contribution is so small that its absence or presence would make an indistinguishable difference in the total spectrum. Consequently, the sensitivity to chiral restoration appears to be very weak.

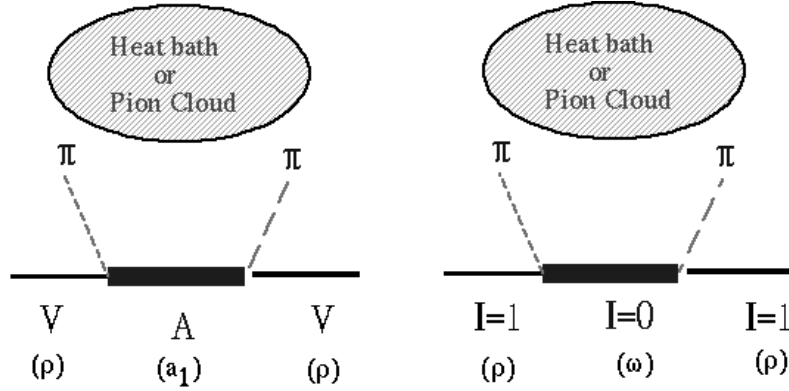


Fig. 1. Schematic illustration of mixing induced by the medium. Left: Vector axial-vector mixing. Right: Iso-vector iso-scalar mixing.

Finally, there has been discussion about the contributions of baryons, notably the  $N(1520)$  resonance [4, 5]. Again, this can be understood either as a mixing of the  $\rho$ -meson with  $N(1520)$ -hole states or simply as the Dalitz decay of the  $N(1520)$ . At present, it is unclear what the chiral properties of a  $N(1520)$ -hole state are. Therefore, one cannot say to which extent this mixing contributes to chiral restoration. However, as will be shown below, the contribution of the  $N(1520)$ -Dalitz again is so small, that it hardly affects the total Dilepton spectrum.

### 3 The $N(1520)$

There has been some discussion as to how important the contribution of baryons to the dilepton spectrum is. Baryon-resonances contribute chiefly through their Dalitz decay  $N^* \rightarrow e^+e^-N$  to the dilepton spectrum. In [6] this contribution has been estimated to be at most 50 % of that of the  $\omega$ -Dalitz decay in the mass range of 400 – 500 MeV. The  $N(1520)$  plays a special role, as it couples very strongly to the  $\rho$  meson and thus should also contribute most to the dilepton spectrum [4, 5]. In order to explore this we have calculated the Dalitz decay rate and width of the  $N(1520)$  using the model and parameters of [7], which is based on an analysis of pion photoproduction data. A detailed description of this calculation can be found in [9]. We have also compared to

the nonrelativistic models, which are usually employed in the calculation of the  $\rho$ -meson spectral function [4, 5]. In fig. 2 we show the resulting width for two relativistic parameterizations and the nonrelativistic result. They agree reasonably well, and in the transport calculations shown below we employ the nonrelativistic result. We should also mention that we found a rather weak dependence on the off-shell parameter, which is always present in the relativistic description of a spin 3/2 object.

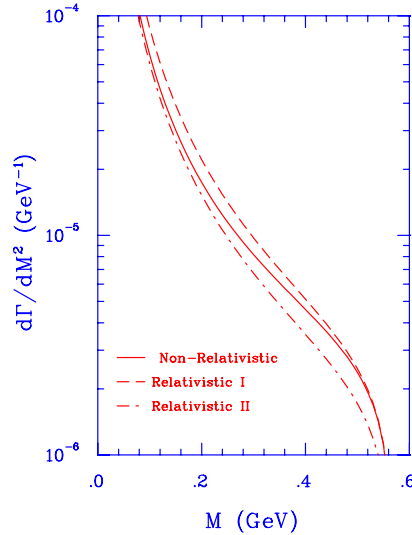


Fig. 2. Dalitz decay width of the  $N(1520)$  based on a relativistic and nonrelativistic descriptions. The difference between the calculations labeled ‘Relativistic I’ and ‘Relativistic II’ are discussed in detail in [9].

## 4 Transport calculation

The results which we will present in the subsequent section are based on a transport calculation. Therefore, it is appropriate to discuss how the dilepton spectrum calculated in transport is related to that obtained from in medium correlation functions (see e.g. [5]). In general, the dilepton production rate is related to the imaginary part of the current-current correlation function  $C(q_0, \vec{q})$

$$\frac{dR}{d^4q} = -\frac{\alpha^2}{\pi^3 q^2} \text{Im } C(q_0, \vec{q}). \quad (1)$$

Assuming vector dominance, and concentrating on the iso-vector vector ( $\rho$ ) channel the current-current correlator is, up to constant factors, given by the

in medium rho propagator  $D_\rho(q_0, \vec{q})$

$$\text{Im } C(q_0, \vec{q}) \sim \text{Im } D_\rho(q_0, \vec{q}) \sim \frac{\text{Im}(\Sigma)}{(m^2 - m_\rho^2 + \text{Re}(\Sigma))^2 + \text{Im}(\Sigma)^2} \quad (2)$$

with

$$\Sigma = \Sigma_{\rho \rightarrow \pi\pi} + \Sigma_{\pi+\rho \rightarrow a_1} + \dots \quad (3)$$

being the selfenergy of the  $\rho$  meson. In free space  $\Sigma = \Sigma_{\rho \rightarrow \pi\pi}$ . In the medium, one gets additional contributions from all the other channels coupling to the  $\rho$  such as the  $a_1$ , the  $\omega$ ,  $N(1520)$  etc.

In transport, on the other hand, one folds the collisions of the respective particles with the branching probability into the dilepton channel in order to generate the dilepton spectrum. At first sight, this appears to be a different approach than the one based on the imaginary part of the correlator. However, the relevant cross sections which control the collision probabilities are directly related to the imaginary part of the selfenergies. Thus the transport calculation can also be formulated in terms of an imaginary part of a correlation function which, for the results shown below has the following form

$$\text{Im } C(q_0, \vec{q})_{\text{transport}} \sim \text{Im } D_\rho(q_0, \vec{q})_{\text{transport}} \sim \frac{\text{Im}(\Sigma)}{(m^2 - m_\rho^2)^2 + \text{Im}(\Sigma_{\rho \rightarrow \pi\pi})^2}. \quad (4)$$

Note that there are two differences between the correlator (2) and that resulting from transport (4). First, in the denominator the real part of the selfenergy is neglected. This is a reasonable approximation as the real part appears to be small [5]. The other approximation is that in the denominator only the free selfenergy enters in the imaginary part. Additional broadening due to other processes is not taken into account. This approximation becomes bad close to the resonance mass, where the imaginary part of the selfenergy dominates the denominator. There, the transport over predicts the actual dilepton yield. However, in the results below we will see that in this region the total dilepton spectrum is dominated by the decay of the  $\omega$  meson, which happens mostly in the final state. Thus, a reduction of the  $\rho$  peak will reduce the overall strength only by a small amount. This effect will become more visible, once the experimental mass resolution becomes sufficiently good to resolve the omega peak. Then the collisional broadening of the  $\rho$  should be directly visible in the neighborhood of the omega. One should also note that this second approximation can in principle be overcome within a transport calculation. The transport gives the full information about the collisional

width ( $Im(\Sigma)$ ) for each spacetime point. It, however, requires a numerical tour de force to do a statistically reliable calculations. While this has not yet been attempted in the framework of nucleus-nucleus collisions, such a calculation has been carried out for dilepton production in photon-nucleus reactions [12].

## 5 Results for Pb+Au at 160 GeV/A and predictions for 40 GeV/A

Let us now turn to the actual results. Most of the details of the calculations can be found in [6]. The new element here is the inclusion of the  $N(1520)$ . In fig. 3 and fig. 4 we show the resulting dilepton spectra in comparison with the preliminary CERES data from 1996 [8]. We find an overall agreement with the data, also for the low transverse momentum ones. Notice, these results have been obtained without any in-medium effects. As explained in [6] the initial conditions have been chosen such that the final hadronic spectra agree with experiment.

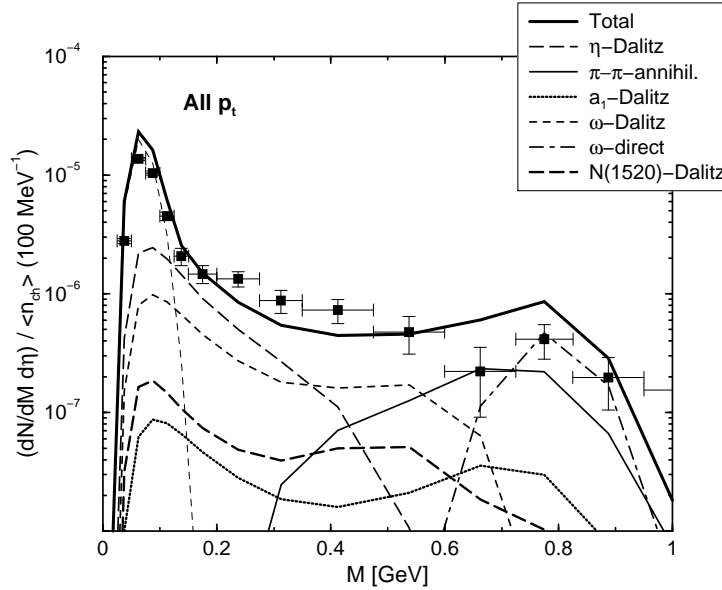


Fig. 3. Results for the dilepton invariant mass spectrum at 160 GeV/A. All transverse momenta. Calculation based on model of [6].

As discussed above, an indicator for the chiral mixing of axial-vector and vector correlator is the  $a_1$  Dalitz contribution (thick full line at the bottom of the graph). In our calculation the  $a_1$ -Dalitz is at best a 2 % contribution. Considering the size of the experimental error bars, it is clear that the present

data do not allow for any conclusions concerning chiral restoration. Note that our findings here are also in agreement with refs. [10] and [11]. Both references find that the  $a_1$ -Dalitz rate is considerably smaller than the pion annihilation rate.

We also find a rather small contribution from the  $N(1520)$  decay (thick dashed line at the bottom of the graph). It is about a factor of 4 below the contribution of the  $\omega$ -Dalitz decay, supporting the early estimate of [6]. This also implies that at least for the 160 GeV data, the contribution of the baryons is rather small.

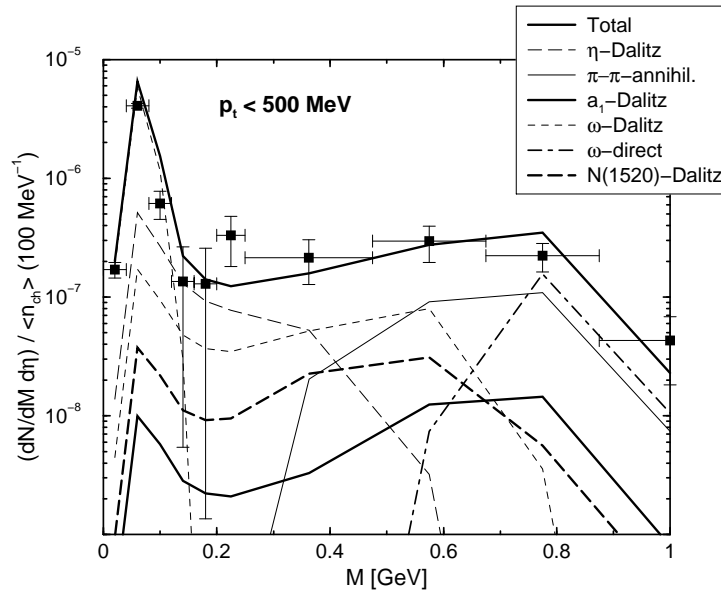


Fig. 4. Results for the dilepton invariant mass spectrum at 160 GeV/A. Transverse momenta below 500 MeV/c. Calculation based on model of [6].

Let us next turn to our prediction for the ‘low energy’ (40 GeV) run. In figs. 5 and 6 we show our prediction together with the 160 GeV data, which are intended as a reference. The prediction is based on central ( $N_{charge} = 220$ ) events generated with URQMD [13] (for details of the calculation see [9]). In our calculation, we have assumed a mass resolution of 1 %, in order to account for the substantially improved mass resolution of the CERES spectrometer. Given this mass resolution, the omega should be clearly visible and thus should put a strong constraint on the model calculations. Aside from the improved resolution, however, we do not predict a significant difference between the high energy and the low energy spectrum, if plotted in the CERES normalization i.e. if divided by the number of charged particles. The only small but visible

difference is around 400 MeV, where the yield is somewhat smaller than that of the high energy run. Finally, we find that the contribution of the baryons is still comparatively small, although somewhat stronger than for the high energy collisions.

We have also carried out a calculation in the spirit of [6], where we have adjusted the initial hadronic state in order to reproduce the final spectra of an RQMD calculation at 40 GeV/A. The results are virtually identical to the ones using the full URQMD events.

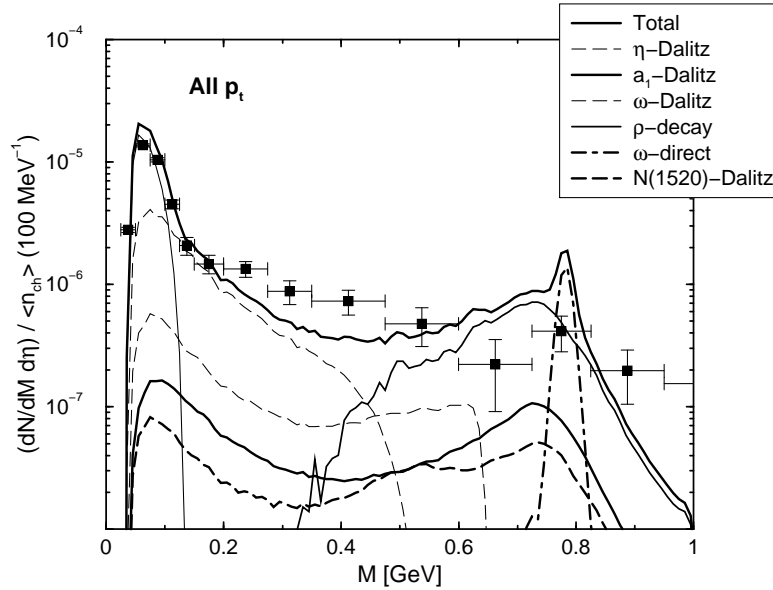


Fig. 5. Prediction for the dilepton invariant mass spectrum for Pb+Pb at 40 GeV/A. All transverse momenta. Calculation based on URQMD [13]. The data are those for 160 GeV/A [8] and shown for comparison only.

## 6 Conclusions

The imaginary part of the iso-vector vector correlator contributes significantly to the dilepton spectrum. Therefore, a dilepton measurement is in principle sensitive to in medium changes of this correlation function, and thus may be utilized to investigate effects of chiral symmetry restoration, at least indirectly. We have argued that the strength of the  $a_1$ -Dalitz decay provides a good measure for the mixing of the vector and axial-vector correlators, which is one way of restoring chiral symmetry. Our analysis of the presently available dilepton data by the CERES collaboration shows a negligible contribution from the  $a_1$ -Dalitz decay, in agreement with other calculations. Therefore, the



present dilepton data do not allow for any conclusions concerning the mixing of the axial-vector and vector correlation functions, and thus about the possible restoration of chiral symmetry achieved in SPS-energy heavy ion collisions.

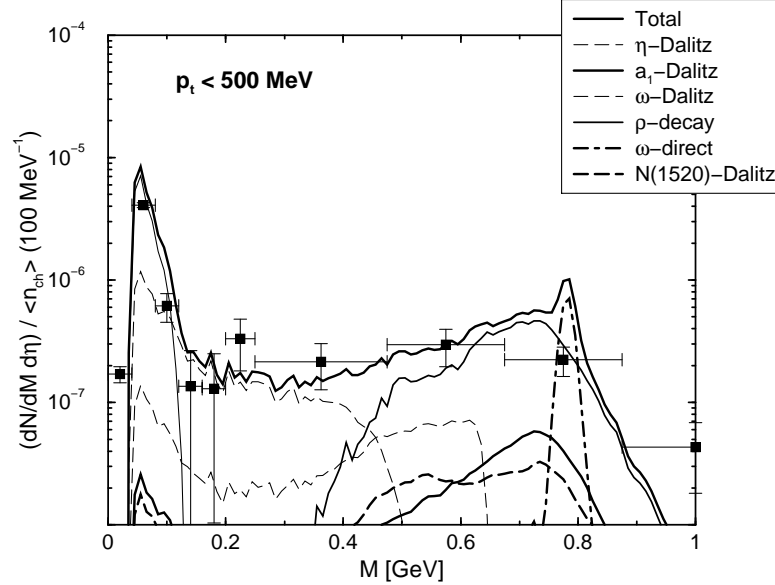


Fig. 6. Prediction for the dilepton invariant mass spectrum for Pb+Pb at 40 GeV/A. Transverse momenta below 500 MeV/c. Calculation based on URQMD [13]. The data are those for 160 GeV/A [8] and shown for comparison only.

We have also provided a prediction for the dilepton spectrum in central Pb+Pb collisions at 40 GeV/A. If normalized by the number of charged particles we find only small differences between the low energy and the high energy spectra. Furthermore, even at the low bombarding energy, we find that the contribution from baryons is rather small.

**Acknowledgments:** The work of CG and AKDM was supported by the Natural Sciences and Engineering Research Council of Canada and the Fonds FCAR of the Québec Government. The work of CMK was supported in part by the National Science Foundation under Grant No. PHY-9509266 and PHY-9870038, the Welch Foundation under Grant No. A-1358, the Texas Advanced Research Program under Grant FY97-010366-068, and the Alexander v. Humboldt Foundation. MB and VK were supported by the Director, Office of Science, Office of High Energy and Nuclear Physics, Division of Nuclear Physics, and by the Office of Basic Energy Sciences, Division of Nuclear Sciences, of the U.S. Department of Energy under Contract No. DE-AC03-76SF00098.

MB was also supported by a Feodor Lynen Fellowship of the Alexander v. Humboldt Foundation, Germany.

## References

- [1] M. Dey, V. L. Eletzky and B. Ioffe, Phys. Lett. **B252** (1990) 620;
- [2] J. I. Kapusta and E. V. Shuryak, Phys. Rev. **D49** (1994) 4694.
- [3] G. Chanfray et al., Nucl. Phys. **A637** (1998) 421.
- [4] W. Peters et al, Nucl. Phys. **A632** (1998) 109.
- [5] R. Rapp et al. Nucl. Phys. **A617** (1997) 472.
- [6] V. Koch and C. Song, Phys. Rev. C **54** (1996) 1903.
- [7] T. Feuster and U. Mosel, Nucl. Phys. **A612**, (1997) 375.
- [8] B. Lenkeit for the CERES Collaboration, (Quark Matter 99, Proc. Int. Conf. on Ultra-Relativistic Nucleus-Nucleus Collisions, Torino, 1999); Nucl. Phys. A661 (1999).
- [9] A. K. Dutt-mazumder et al, in preparation.
- [10] K. Haglin, Phys. Rev. **C53** (1996) 2606.
- [11] R. Rapp and C. Gale, Phys. Rev. C **60**, (1999) 024903 .
- [12] M. Effenberger et al., Phys. Rev. C. **60** (1999) 044614 64.
- [13] S. A. Bass et al, Prog. Part. Nucl. Phys. **41** (1998) 225; M. Bleicher et al, J. Phys. G **25** (1999) 1859.